



# Smooth surfaces, umbilics, lines of curvatures, foliations, ridges and the medial axis: a concise overview

Frédéric Cazals, Marc Pouget

## ► To cite this version:

Frédéric Cazals, Marc Pouget. Smooth surfaces, umbilics, lines of curvatures, foliations, ridges and the medial axis: a concise overview. RR-5138, INRIA. 2004. [inria-00071445](https://hal.inria.fr/inria-00071445)

**HAL Id: [inria-00071445](https://hal.inria.fr/inria-00071445)**

**<https://hal.inria.fr/inria-00071445>**

Submitted on 23 May 2006

**HAL** is a multi-disciplinary open access archive for the deposit and dissemination of scientific research documents, whether they are published or not. The documents may come from teaching and research institutions in France or abroad, or from public or private research centers.

L'archive ouverte pluridisciplinaire **HAL**, est destinée au dépôt et à la diffusion de documents scientifiques de niveau recherche, publiés ou non, émanant des établissements d'enseignement et de recherche français ou étrangers, des laboratoires publics ou privés.

*Smooth surfaces, umbilics, lines of curvatures,  
foliations, ridges and the medial axis: a concise  
overview*

Frédéric Cazals — Marc Pouget

**N° 5138**

Mars 2004

THÈME 2



*Rapport  
de recherche*



## Smooth surfaces, umbilics, lines of curvatures, foliations, ridges and the medial axis: a concise overview

Frédéric Cazals, Marc Pouget

Thème 2 — Génie logiciel  
et calcul symbolique  
Projet Geometrica

Rapport de recherche n° 5138 — Mars 2004 — 27 pages

**Abstract:** The understanding of surfaces embedded in  $\mathbb{R}^3$  requires local and global concepts, which are respectively evocative of differential geometry and differential topology. While the local theory has been classical for decades, global objects such as the foliations defined by the lines of curvature, or the medial axis still pose challenging mathematical problems. This duality is also tangible from a practical perspective, since algorithms manipulating sampled smooth surfaces (meshes or point clouds) are more developed in the local than the global category. As an example and assuming this makes sense for the applications encompassed, we are not aware as of today of any algorithm able to report —under reasonable assumptions— a topologically correct medial axis or foliation from a sampled surface.

As a prerequisite for those interested in the development of algorithms for the manipulation of surfaces, we propose a concise overview of global objects related to curvature properties of a smooth generic surface. Gathering from differential topology and singularity theory sources, our presentation focuses on the geometric intuition rather than the technicalities. We first recall the classification of umbilics, of curvature lines, and describe the corresponding stable foliations. Next, fundamentals of contact and singularity theory are recalled, together with the classification of points induced by the contact of the surface with a sphere. This classification is further used to define ridges and their properties, and to recall the stratification properties of the medial axis.

From a theoretical perspective, we expect this survey to ease the access to intricate notions scattered over several sources. From a practical standpoint, we hope it will be helpful for those interested in the manipulation of surfaces without using global parametrizations, and also for those aiming at producing globally coherent approximations of surfaces.

**Key-words:** Smooth surfaces, Differential Geometry, Umbilics, Lines of Curvatures, Foliations, Ridges, Medial Axis.

## **Surfaces lisses, ombilics, lignes de courbure, feuilletages, extrêmes de courbure et axe médian: un panorama concis**

**Résumé :** La compréhension des surfaces plongées dans  $\mathbb{R}^3$  nécessite des concepts locaux et globaux, ceux-ci évoquant respectivement la géométrie différentielle et la topologie différentielle. Alors que la théorie locale est classique depuis des décennies, les aspects globaux tels que les feuilletages définis par les lignes de courbure, ou l'axe médian posent toujours des problèmes mathématiques difficiles. Cette dualité est aussi perceptible d'un point de vue pratique, puisque les algorithmes manipulant des surfaces lisses échantillonnées (maillages ou nuages de points) sont plus développés pour les aspects locaux que globaux. Par exemple, en supposant que cela ait un sens pour les applications considérées et sous des hypothèses raisonnables, il n'existe pas à notre connaissance d'algorithme capable de calculer l'axe médian ou un feuilletage d'une surface échantillonnée avec des garanties topologiques.

À l'intention de ceux qui s'intéressent au développement d'algorithmes pour la manipulation de surfaces, nous proposons un panorama concis des objets globaux relatifs aux propriétés de courbure d'une surface lisse générique. À partir d'éléments de topologie différentielle et de théorie des singularités, notre présentation met l'accent sur l'intuition géométrique plus que sur les aspects techniques. En premier lieu, nous rappelons la classification des ombilics, des lignes de courbure, et décrivons les feuilletages stables correspondants. Ensuite, nous introduisons les bases de la théorie du contact et des singularités, ainsi que la classification des points induite par le contact de la surface avec un sphère. Cette classification est utilisée pour définir les extrêmes de courbure et leur propriétés, et pour décrire la stratification de l'axe médian.

Sur le plan théorique, nous espérons ainsi faciliter l'accès à des notions disséminées dans des sources variées. Sur le plan pratique, ce panorama sera certainement utile à ceux qui s'intéressent à la manipulation de surfaces sans paramétrage global, ainsi qu'à ceux qui cherchent à obtenir des approximations globalement cohérentes de surfaces.

**Mots-clés :** Surfaces Lisses, Géométrie différentielle, Ombilics, Lignes de Courbure, Feuilletages, Extrêmes de courbure, Axe Médian.

# 1 Introduction

## 1.1 Global differential patterns

Sampled surfaces represented either by point clouds or meshes are ubiquitous in computer graphics, computer aided design, medical imaging, computational geometry, finite element methods or geology. Aside from the situations where a sample surface is of self-interest —e.g. in computer graphics, sampled surfaces approximating (piecewise-)smooth surfaces are essentially found in two contexts which are surface reconstruction and surface discretization. In the first category, one is given a set of sample points acquired from a scanner (medical or laser) and wishes to reconstruct (by interpolation or approximation) the continuous or (piecewise-)smooth surface which has been sampled. In the second one, a surface is given implicitly or parametrically, and one wishes to discretize it for visualization or calculation purposes. In any case, three types of properties are usually of interest when comparing a (piecewise-)smooth surface and its discretization: topological and geometric properties, local differential properties, and global differential properties.

From a topological standpoint, one expects the surfaces to be homeomorphic or even better isotopic. Example algorithms with such a guarantee are [AB99, ACDL00] in the surface reconstruction area, and [BCSV04, BO03] in the surface meshing context. (The claims made for the surface reconstruction algorithms is about homeomorphy, although isotopy actually holds.) Apart from these algorithms, the interested reader should consult [PS03, CCs04] where sufficient conditions on isotopy can be found. It should also be pointed out that the hypothesis under which one achieves these properties usually also yield a bound on the Hausdorff distance between the surfaces, a property of geometric nature.

Local differential properties are of two types, namely intrinsic and extrinsic. For extrinsic quantities, one wishes to guarantee that the tangent plane (at the first order), the principal directions and curvatures (at the second order), or higher order coefficients (e.g. extremality coefficients) are close. The development of algorithms providing such guarantees has been subject to intense research [Pet01], and recent advances provide guarantees either point-wise [BCM03, CP03] or in the geometric measure theory sense [CSM03]. Although extrinsic properties are usually the properties sought, some applications care for intrinsic faithfulness. These applications are usually concerned with the question of flattening / parameterizing a surface, and the reader is referred to [MT01] for an example related to geology, together with the ensuing conditions.

At last, global differential properties usually refer to guarantees on loci of points having a prescribed differential property. Example such loci are lines of curvature, ridges, or the medial axis. Applications involving such patterns are surface remeshing [ACSD<sup>+</sup>03], scientific visualization [DH94], feature extraction [PAT00, WB01, HGY<sup>+</sup>99], or surface reconstruction [AB99, BC01] and related topics [DZ02, Lie03]. Providing such guarantees cumulates the difficulties afore-mentioned. Not only point-wise estimates must be reliable, but they must also be connected correctly at the surface level. This difficulties are tangible from a practical perspective, and to the best of our knowledge, no algorithm as of today is able to report any global differential pattern with some guarantee.

This is partly due to the fact that global differential patterns have an involved structure described in differential topology and singularity theory sources. Easing the access to these notions is the

incentive of this concise survey, whose presentation focuses on the geometric intuition rather than the technicalities. From a practical standpoint, we hope it will be helpful for those interested in the manipulation of surfaces without using charts, and also for those aiming at producing globally coherent approximations of surfaces.

## 1.2 An example: the ellipsoid

With some anticipation and as an appetizer, we illustrate the global structure theorems we are aiming at on the famous example of an ellipsoid with three different axes. Figures 1 and 2 are produced by the algorithm described in [CP04]. Principal curvatures are sorted, that is  $k_1 \geq k_2$ , and objects related to the larger (smaller) principal curvature are painted in blue or green (red or yellow). As an example on Fig. 1, the blue principal direction field is drawn —from which one infers that the normal is pointing outward so that the two principal curvatures are negative.

Blue elliptic ridges are blue, blue hyperbolic are green. Red elliptic ridges are red, red hyperbolic are yellow. Intersections between ridges are the purple points. The two elliptic ridges are closed curves without turning point. The four Lemon umbilics are the black dots, and they are linked by four separatrices —the yellow and green curves. The separatrices, which are curvature lines, are also ridges in that case. More generally, any line of symmetry is a line of curvature and a ridge ([Por01, p.162]). Notice also that the lines of curvatures which are not separatrices are all cycles. For each color, they are packed into a cylinder. But this is a non stable configuration since separatrices are umbilical connections, the cycles are not hyperbolic. The medial axis of the ellipsoid is a region homeomorphic to a disk, and is located in the symmetry plane of the two largest axes. This region looks like an ellipsis but is not so [Deg97]. The boundary of the medial axis projects onto the red ridge curve, and reciprocally on this example, every elliptic red ridge point corresponds to a point on the boundary of the medial axis.

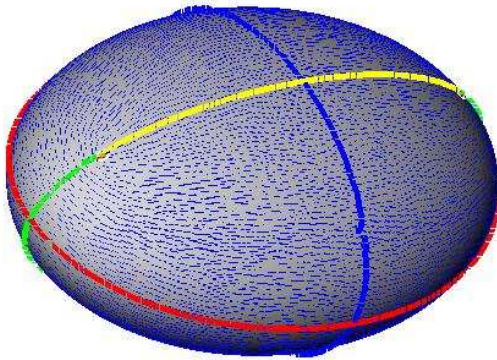


Figure 1: Umbilics, ridges, and principal blue foliation on the ellipsoid

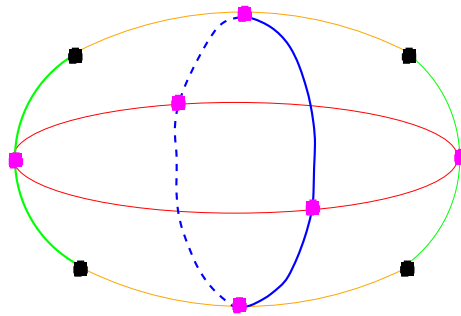


Figure 2: Schematic view of the umbilics and the ridges. Max of  $k_1$ : blue; Min of  $k_1$ : green; Min of  $k_2$ ; Max of  $k_2$ : yellow

### 1.3 Paper overview

In section 2, the Monge form of a surface is recalled. Second order properties —umbilics and lines of curvature— are presented in section 3. The classification of contact points between the surface and spheres is presented in section 4. This classification is used in section 5 to recall the stratification properties of the medial axis.

## 2 The Monge form of a surface

### 2.1 Generic surfaces

Our focus is on generic phenomena on surfaces, and the statements presented are valid for generic surfaces only. Formally if one considers the set of all smooth surfaces  $M$  in  $\mathbb{R}^3$  as an infinite dimensional space, a property is generic if the surfaces exhibiting this property form an open dense subset. Informally this notion means that only generic properties are stable if one allows small random perturbations.

In the particular description of surfaces as Monge patches, we have a family of Monge patches with 2 degrees of freedom. A property requiring 1 (resp. 2) condition(s) on this family is expected to appear on a lines (resp. isolated points) of the surface. A property requiring at least 3 conditions is not generic.

### 2.2 The Monge form of a surface

We consider a surface  $S$  embedded in the Euclidean space  $E^3$  equipped with the orientation of its world coordinate system —referred to as the *direct orientation* in the sequel. At any point of the surface which is not an umbilic, principal directions are well defined, and the (non oriented) principal directions  $d_{max}$ ,  $d_{min}$  together with the normal vector  $n$  define two direct orthonormal frames. If  $v_1$  is a vector of direction  $d_{max}$  then there exists a unique  $v_2$  so that  $(v_1, v_2, n)$  is direct; and the other possible frame is  $(-v_1, -v_2, n)$ . In one of these, and as long as our study is a local differential one, the surface is assumed to be given as a Monge patch at the origin [HGY<sup>+</sup>99] —with *h.o.t* standing for *higher order terms*:

$$z = \frac{1}{2}(k_1x^2 + k_2y^2) + \frac{1}{6}(b_0x^3 + 3b_1x^2y + 3b_2xy^2 + b_3y^3) \\ + \frac{1}{24}(c_0x^4 + 4c_1x^3y + 6c_2x^2y^2 + 4c_3xy^3 + c_4y^4) + h.o.t$$

Occasionally, we shall refer to the cubic part  $C_M(x, y)$  as the Monge cubic, that is:

$$C_M(x, y) = b_0x^3 + b_1x^2y + b_2xy^2 + b_3y^3. \quad (1)$$

If the origin is not an umbilic, the principal direction associated to  $k_1$  (resp.  $k_2$ ) is the  $x$  (resp.  $y$ ) axis. We shall always assume that  $k_1 \geq k_2$  and we consider 'blue' (resp. 'red') something special



happening with  $k_1$  (resp.  $k_2$ ). For example the blue focal surface is the set of centers of curvature associated to the blue curvature  $k_1$ . Note that a change of the normal surface orientation swaps the colors.

Away from umbilics, local analysis of the principal curvatures can be done for the Monge coordinate system and along the curvature lines. The Taylor expansion of the principal curvature  $k_1$  in the Monge coordinate system is

$$k_1(x, y) = k_1 + b_0x + b_1y + \left(\frac{c_0 - 3k_1^2}{2} + \frac{b_1^2}{k_1 - k_2}\right)x^2 \quad (2)$$

$$+ \left(c_1 + \frac{2b_1b_2}{k_1 - k_2}\right)xy + \left(\frac{c_2 - k_1k_2^2}{2} + \frac{b_2^2}{k_1 - k_2}\right)y^2 + h.o.t \quad (3)$$

The Taylor expansion of  $k_1$  (resp.  $k_2$ ) along the blue (resp. red) curvature line going through the origin and parameterized by  $x$  (resp.  $y$ ) are:

$$k_1(x) = k_1 + b_0x + \frac{P_1}{2(k_1 - k_2)}x^2 + h.o.t \quad P_1 = 3b_1^2 + (k_1 - k_2)(c_0 - 3k_1^2). \quad (4)$$

$$k_2(y) = k_2 + b_3y + \frac{P_2}{2(k_2 - k_1)}y^2 + h.o.t \quad P_2 = 3b_2^2 + (k_2 - k_1)(c_4 - 3k_2^3). \quad (5)$$

Notice also that switching from one of the two coordinate systems mentioned in introduction to the other reverts the sign of all the odd coefficients on the Monge form of the surface.

Some notions about cubics will be useful in the sequel.

**Definition. 1** A real cubic  $C(x, y)$  is a bivariate homogeneous polynomial of degree three, that is  $C(x, y) = b_0x^3 + 3b_1x^2y + 3b_2xy^2 + b_3y^3$ . Its discriminant is defined by  $\delta(C) = 4(b_1^2 - b_0b_2)(b_2^2 - b_1b_3) - (b_0b_3 - b_1b_2)^2$ .

A cubic factorizes as a product of three polynomials of degree one with complex coefficients, called its factor lines. In the  $(x, y)$  plane, a real factor line defines a direction along which  $C$  vanishes. The number of real factor lines depends on the discriminant of the cubic and we have —notice that  $\delta = 0$  is not discussed since we care for generic events:

**Proposition. 1** Let  $C$  be a real cubic and  $\delta$  its discriminant. If  $\delta > 0$  then there are 3 distinct real factors, else  $\delta < 0$  and there is only one real factor.

### 3 Umbilics and lines of curvature, principal foliations

This section is devoted to second order properties on a surface, and more precisely to umbilics and lines of curvature. General references are [Mor90, Por01, GS91, HGY<sup>+</sup>99].

### 3.1 Classification of umbilics

To present the classification of umbilics, let us first recall some facts about lines of curvature. On each point of the set  $S'$  defined as the surface  $S$  except its umbilics, the two principal directions are well defined and orthogonal. They define two line or direction fields on  $S'$ , one everywhere orthogonal to the other, so it is sufficient to study only one of these. Each principal direction field defines lines of curvature. The set of all these lines, called the principal foliation, will be studied in the next section.

**Definition. 2** *A line of curvature is an integral curve of the principal field, that is a regular curve on  $S'$  which is everywhere tangent to the principal direction and is maximal for inclusion (it contains any regular curve with this property which intersects it).*

The index of an umbilic describes the way the lines of curvature turn around the umbilic. The index of a direction field at a point is  $(1/2\pi) \int_0^{2\pi} \theta(r) dr$ , where  $\theta(r)$  is the angle between the direction of the field and some fixed direction, and the integral is taken over a small counterclockwise circuit around the point. For generic umbilics this index is  $\pm 1/2$ , this implies that the direction field is not orientable on a neighborhood of such points. As illustrated on Fig. 3.1, if one fixes an orientation of the field at a point on a circuit around an umbilic, propagating this orientation by continuity along the circuit gives the reverse orientation after one turn. In other words, there is no non vanishing continuous vector field inducing the direction field around the umbilic. The index can also be computed with the Monge cubic, this computation is point wise as opposed to the previous one, but need third order coefficients (hence it is likely to be less stable in practice). Let  $S = (b_0 - b_2)b_2 - b_1(b_1 - b_3)$ ,

- if  $S < 0$  then the index is  $-1/2$  and the umbilic is called a star,
- if  $S > 0$  then the index is  $+1/2$  and we have to do more calculations to distinguish between the so called lemon and monstar.

A finer classification is required to distinguish between the two umbilics of index  $+1/2$ . We shall need the following:

**Definition. 3** *Consider an umbilic  $p$  and denote  $T_p S$  the tangent plane of the surface at  $p$ . A limiting principal direction is a direction of  $T_p S$  which is tangent to a line of curvature which end at the umbilic.*

Limiting principal directions are related to the Jacobian cubic of the umbilic (cf. [HGY<sup>+</sup>99]):

$$J_C = B_0 x^3 + 3B_1 x^2 y + 3B_2 x y^2 + B_3 y^3 = b_1 x^3 + (2b_2 - b_0) x^2 y - (2b_1 - b_3) x y^2 - b_2 y^3. \quad (6)$$

The real factor lines of this form are the limiting principal directions at the umbilic. As recalled by proposition 1, the number of such directions depends on the discriminant  $U$  of  $J_C$ :

- If  $U < 0$  then there is one limiting principal direction, necessarily  $S > 0$  and the umbilic is called a lemon.

- If  $U > 0$  then there are three limiting principal directions, furthermore if  $S < 0$  the umbilic is a star else  $S > 0$  and it is called a monstar. For a monstar, the three directions are contained within a right angle and all the curvature lines in this angle end at the umbilic and form the parabolic sector of the monstar. Note that all these lines have the same tangent at the umbilic: the limiting principal direction inside the parabolic sector. For a star, only three lines of curvature end at the umbilic and the limiting directions are not contained in a right angle.

We summarize the previous discussion as follow:

**Theorem. 1** *There are three classes of generic umbilics, namely Lemons, Monstar and Stars. They are distinguished by their index and the number of limiting principal directions.*

A generic umbilic is a non flat point: its Gaussian curvature does not vanish —since it is a third condition on the Monge patch for a single point. Moreover, Generic umbilics are isolated (cf. [Por01, p.184]).

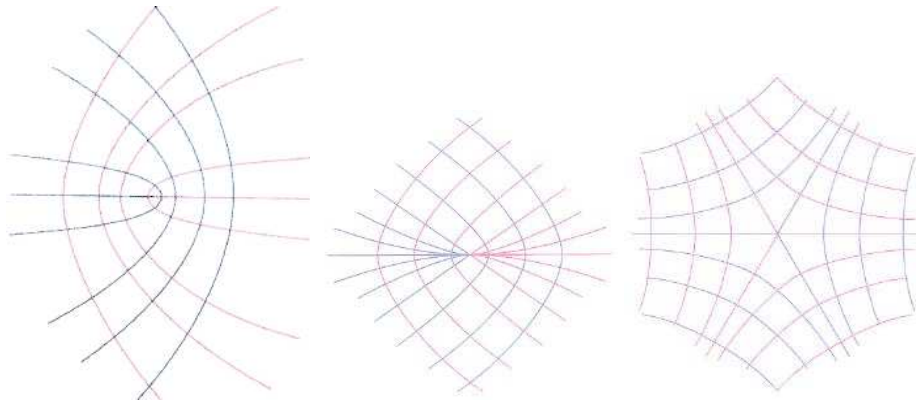


Figure 3: Umbilics: Lemon and Monstar of index  $+1/2$ , Star of index  $-1/2$ . Figure from [Por01]

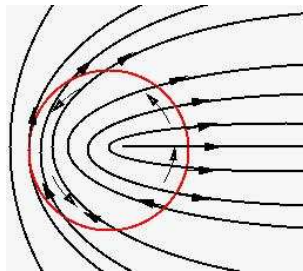


Figure 4: Impossibility of a global orientation around an umbilic

### 3.2 Principal foliations

Having classified umbilics, let us get back to the principal foliations. Recall that the blue (resp. red) principal foliation is the set of all blue (resp. red) curvature lines defined on  $S'$ . The umbilics can be regarded as singular points for these foliations if one wishes to consider them on  $S$ . The first element required concerns the topology of a curvature line. A line of curvature  $\gamma$  is either homeomorphic to:

- the real line  $\mathbb{R}$ , then it can be oriented and parameterized by arc length on its maximal interval  $I = (\omega_-, \omega_+)$ . Its  $\alpha(\gamma)$  (resp.  $\omega(\gamma)$ ) limit set is the collection of limit points of sequences  $\gamma(s_n)$ , convergent in  $S$ , with  $s_n$  tending to  $\omega_-$  (resp.  $\omega_+$ ). The limit set of  $\gamma$  is the union  $\alpha(\gamma) \cup \omega(\gamma)$ .
- or to a circle, then it is called a cycle. It is hyperbolic if its Poincaré return map  $\pi$  is so that  $\pi' \neq 1$ . In other words, if one orients an hyperbolic cycle, the lines of curvature can be oriented on a neighborhood of this cycle by continuity and they are all attracted or repelled on both sides of the cycle (cf. Fig. 3.2).

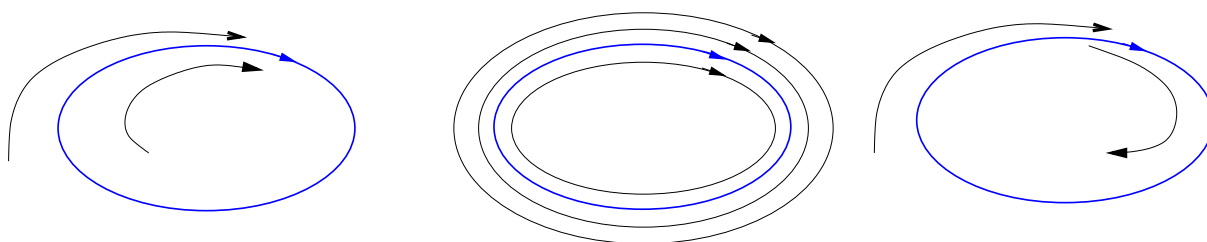


Figure 5: A hyperbolic cycle and two non hyperbolic ones

Special lines divide the set of all curvature lines in the vicinity of an umbilic into sectors, they are separatrices.

**Definition. 4** A *separatrix* is a line of curvature with an umbilic in its limit set and so that there exists arbitrarily close to that line, another line without this umbilic in its limit set.

A sector defined by two consecutive separatrices is

- hyperbolic if none of the lines in the sector have the umbilic in their limit set;
- parabolic if all curvature lines in the sector have the umbilic in their  $\alpha$  or exclusive  $\omega$  limit set;

The alternative case of an elliptic sector, if all curvature lines in the sector have the umbilic in their  $\alpha$  and  $\omega$  limit set, is not generic —cf. Nikolaev [Nik01, p.360]. Note that a separatrix is a line of curvature which ends at an umbilic, hence its tangent at this point is a limiting principal direction. But the limiting principal direction inside the parabolic sector of a monstar is not tangent to

a separatrix of this umbilic —because all lines in a neighborhood have the monstar in their limit set. This explains another classification of umbilics from Darboux based on the number of separatrices. This classification rephrases the previous one: a lemon or  $D_1$  has one separatrix, a monstar or  $D_2$  has two and a star or  $D_3$  has three.

The next result [GS91, p.27] describes stable configuration of the principal foliations for a smooth compact oriented surface given by an immersion.

**Theorem. 2** *Let  $\Sigma$  be the subset of smooth compact oriented surfaces which satisfies the following four conditions:*

- *all the umbilic points are of type  $D_{i,i=1,\dots,3}$ ;*
- *all the cycles are hyperbolic;*
- *the limit sets of every line of curvature are umbilics or cycles;*
- *all the separatrices are separatrices of a single umbilic (they cannot connect two umbilics or twice the same one being separatrices at both ends).*

*Then  $\Sigma$  is open and each of its elements is structurally stable in the  $C^3$ -sense,  $\Sigma$  is dense in the  $C^2$ -sense.*

This theorem implies that stable principal foliations on generic surfaces are described with the set of umbilics, cycles and the way the separatrices connect these elements. The complement of these features on the surface  $S$  then decomposes on canonical regions of two types parallel and cylindrical. On each region, the limit sets of all lines are the same: a cycle or a  $D_2$  umbilical point (through its parabolic sector). A region is parallel if there are separatrices in its boundary. If the boundary consists only of cycles then the region is cylindrical.

If we study a compact surface  $S$ , the topology implies a constraint on the number and the type of umbilics. More precisely, the sum of indices of umbilics must be the Euler characteristic  $\chi(S)$  —[Spi99, p.223]. Moreover, the principal foliation defines a bipartite graph  $G(V_1, V_2, E)$  with  $V_1$  the set of umbilics,  $V_2$  the set of cycles and parabolic sectors and  $E$  the set of separatrices. The edges connect elements of  $V_1$  to elements of  $V_2$  with the following constraints.

- A  $D_i$  umbilic has  $i$  incident edges,
- Since there is no elliptic sector, a separatrix of a  $D_2$  umbilic cannot be connected to its parabolic sector,
- The graph is embedded on the surface without intersecting the separatrices.

## 4 Contacts of the surface with spheres, Ridges

To classify points of a smooth surface regarding curvature properties, we first recall fundamentals from contact and singularity theory. Following [Por71, Por83, Mor90], we probe a point of the surface with a sphere centered along the normal at that point. Working out the dominant terms of the Taylor expansion of the probe function yields the classification of points desired. General references for this section are [BG92], [Por01] or [Arn92].

### 4.1 Distance function and contact function

A standard way to classify points on a smooth surface consists of using contact theory. Consider a portion of surface locally parameterized in a chart  $(U, p(x, y))$  with  $U \subset \mathbb{R}^2$ ,  $(x_0, y_0) \in U$  and a sphere  $C$  of center  $c$ . The contact function at the point  $p(x_0, y_0) \in S$  is the function defined by:

$$g : U \times \mathbb{R}^3 \mapsto \mathbb{R}, g((x, y), c) = \langle p(x, y), c \rangle^2 - \langle p(x_0, y_0), c \rangle^2.$$

This function is just the square distance from the surface to the center of the sphere minus the square of its radius  $r^2 = \langle p(x_0, y_0), c \rangle^2$ . The intersection points between  $S$  and  $C$  have coordinates  $(x, y, p(x, y))$  satisfying  $g(x, y) = 0$ . The philosophy of contact theory is the following. Once the center of the sphere have been chosen, the contact function is a bivariate function. Then, we wish to report the possible *normal forms* of  $g$  as a bivariate function.

Before illustrating this process, let us observe that if the center of the sphere  $C$  is not contained in the affine space defined by the contact point and the normal at the surface  $S$  there, then the intersection between  $S$  and  $C$  is transverse, which does not reveal much about  $S$  at  $p$ . Studying the nature of the contact really starts with a center aligned with the normal, and we shall see that the cases encountered actually yield a decomposition of the normal bundle<sup>1</sup> of the surface.

**Rmk 1** *Note that if one of the principal curvature vanishes, one can assume the center of the principal sphere is at infinity. This means that the relevant contact to be considered is that of a plane with the surface at such a point. One can find a precise description of these parabolic points in [HGY<sup>+</sup>99].*

### 4.2 Generic contacts between a sphere and a surface

Before presenting the generic contacts, let us illustrate the process of finding the first normal form using the Morse lemma. To ease the calculations, assume that the contact point is the origin, that the surface is given in Monge form, and that the center of the sphere has coordinates  $c(0, 0, r)$ . Then, the contact function simplifies to:

$$g(x, y) = x^2 + y^2 + (z - r)^2 - r^2 = \langle pc, pc \rangle - r^2. \quad (7)$$

<sup>1</sup>The normal bundle of the surface is the three-dimensional manifold obtained by adding to each point of the surface a one-dimensional affine space defined by the pair (point, normal).

Using the Monge form of  $f$ , one gets the following expansion:

$$g(x,y) = x^2(1 - rk_1) + y^2(1 - rk_2) - \frac{r}{3}C_M(x,y) + h.o.t \quad (8)$$

The expansion does not contain linear terms and the origin is therefore a critical point. Moreover, if  $r \neq 1/k_1$  and  $r \neq 1/k_2$ , the critical point is non-degenerate. By the Morse lemma, the contact function rewrites as  $g = \pm x^2 \pm y^2$  up to a diffeomorphism. If the coefficients of both variables have the same sign, then the intersection between  $S$  and  $C$  reduces to point. Otherwise, the intersection consists of two curves.

The previous discussion is typical from singularity theory. Assuming  $r \neq 1/k_1$  and  $r \neq k_2$ , we worked out the the *normal* form of a multivariate function, thus highlighting its dominant terms. In the sequel, we shall just state and use the classification of generic singularities of the contact function. As illustrated by Morse's lemma, it is important to observe that the normal form is exact, i.e. does not hide any higher order term. We shall need the following:

**Definition. 5** Let  $f(x,y)$  be a smooth bivariate function. Function  $f$  has an  $A_k$  or  $D_k$  singularity if, up to a diffeomorphism, it can be written as:

$$\begin{cases} A_k : f = \pm x^2 \pm y^{k+1}, k \geq 0, \\ D_k : f = \pm yx^2 \pm y^{k-1}, k \geq 4. \end{cases} \quad (9)$$

The singularity is further denoted  $A_k^\pm$  or  $D_k^\pm$  if the product of the coefficients of the monomials is  $\pm 1$ .

As subsumed by this definition, an  $A_k$  singularity precludes an  $A_{k+1}$  singularity, and similarly for  $D_k$ . An important characteristic of these normal forms is their zero level set. Those of the  $A_k$  sequence are illustrated on Fig. 6, where the (branches of) curves are defined from  $x = \pm y^{(k+1)/2}$ . More precisely:

**Observation. 1** The zero level set of an  $A_0$  singularity consists of a smooth curve, and that of an  $A_{2p}$  singularity for  $p \geq 1$  consists of one curve having a cusp at the origin. The zero level set of an  $A_{2p-1}$  singularity consists consists of two tangential curves or an isolated point depending on the product of the signs of the monomials.

For a  $D_k$  singularity, since  $f = y(\pm x^2 \pm y^{k-2})$ , the line  $y = 0$  is always solution. For the other solutions, the discussion is identical to the  $A_k$  case.

**Observation. 2** The zero level set of an  $D_{2p}^+$  ( $D_{2p}^-$ ) singularity consists of one (three) curve(s). The zero level set of an  $D_{2p+1}^+$  or  $D_{2p+1}^-$  singularity consists of two curves.

The classification of generic contact points is the following [Por71, Por83]:

**Theorem. 3** The generic singularities of the contact function between a sphere and a surface are of type  $A_0, A_1, A_2, A_3, A_4, D_4$ .

The  $A_0$  contact is just the transverse intersection mentioned at the beginning of this section, and we shall not discuss it further. The others types of contacts —respectively  $A_k$  and  $D_k$ — encode properties of the surface away from umbilics and at umbilics.

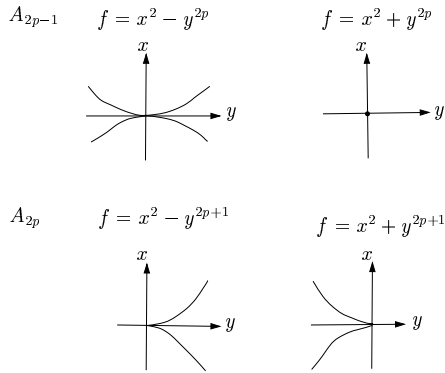


Figure 6: Zero level sets of the  $A_k : f = x^2 \pm y^{k+1}$  singularities

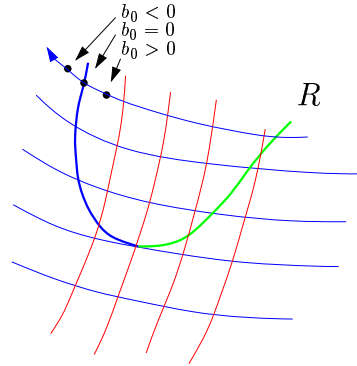


Figure 7: Variation of the  $b_0$  coefficient and turning point of a ridge

### 4.3 Contact points away from umbilics

We proceed with the discussion of the contacts away from umbilics.

**$A_1$  contact.** [ $r = 1/k_1, r \neq 1/k_2$ ] The origin is a non degenerate critical point. The intersection reduces to one point or consists of two curves depending on the value of  $r$  wrt  $1/k_2$  and  $1/k_2$ .

**$A_2$  contact.** [ $r = 1/k_1, b_0 \neq 0$  (or  $r = 1/k_2, b_3 \neq 0$ )] The sphere is a sphere of principal curvature, and the curvature is not an extremum by Eq. (4) since  $b_0 \neq 0$ . Due to the presence of terms of odd degree in the normal form, the intersection between the sphere and the surface is not reduced to a point (cf. Fig. 8 and 9).

**$A_3$  contact.** [ $r = 1/k_1, b_0 = 0, P_1 \neq 0$  (or  $r = 1/k_2, b_3 = 0, P_2 \neq 0$ )] The sphere is a sphere of principal curvature, and the principal curvature has a local extremum since  $b_0 = 0$  and  $P_1 \neq 0$  — or  $b_0 = 3$  and  $P_2 \neq 0$ . An  $A_3$  contact defines a *ridge* point, but not all ridge points are  $A_3$  points. Distinguishing further between  $A_3^-$  and  $A_3^+$  yields the distinction between elliptic and hyperbolic ridge points<sup>2</sup>:

<sup>2</sup>Elliptic and hyperbolic ridge points are called sterile and fertile by Porteous. This refers to the possibility for umbilics to appear near such ridges.



- Elliptic. If  $P_1 < 0$ , the contact function has  $A_3^+$  singularity and its normal form is  $g = y^2 + x^4$ . Equivalently, the blue curvature is maximal along its curvature line. The blue sphere of curvature has a local intersection with  $M$  reduced to  $p$  (cf. Fig. 10).
- Hyperbolic. If  $P_1 > 0$ , the contact function has an  $A_3^-$  singularity and its normal form is  $g = y^2 - x^4$ . Equivalently, the blue curvature is minimal along its line. The local intersection of the blue sphere of curvature with  $M$  is two tangential curves (cf. Fig. 11).

For a red ridge point ( $b_3 = 0$ ), we have to consider the quantity  $P_2$  defined by Eq. (5). A red ridge is elliptic if  $k_2$  is minimal ( $P_2 < 0$ ) along its curve and hyperbolic if  $k_2$  is maximal ( $P_2 > 0$ ). (Notice that in Eq. (5) the sign of  $P_2$  is in accordance with the negative sign of  $k_2 - k_1$ .)

Notice that the type, elliptic or hyperbolic, is independent of the surface orientation. Ridge points are on smooth curves on the surface called ridge lines and can be colored according to the color of the points. Away from umbilics, a blue ridge can cross a red ridge at a ridge point colored blue and red that we call a purple point. A crossing of ridges of the same color is not generic.

**$A_4$  contact.** [ $r = 1/k_1, b_0 = 0, P_1 = 0$  (or  $r = 1/k_2, b_3 = 0, P_2 = 0$ )] The blue curvature has a inflection along its line ( $k'_1 = k''_1 = 0$  but  $k'''_1 \neq 0$ , derivatives shall be understood as along the curvature line, cf Eq. (4). As an  $A_4$  singularity, the local intersection of the blue sphere of curvature with  $M$  is a curve with a cusp at the contact point. Such a point is called a *ridge turning point*. At such a point, the ridge is tangent to the line of curvature of the same color, and the ridge changes from elliptic to hyperbolic—from a maximum to a minimum of the principal curvature.

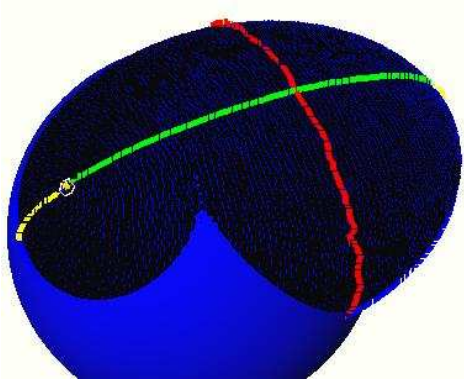
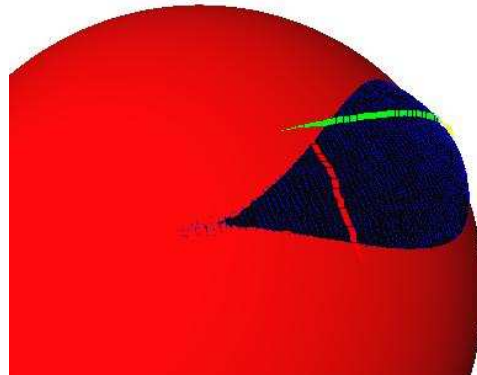
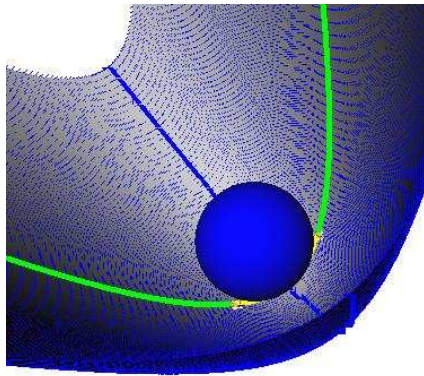
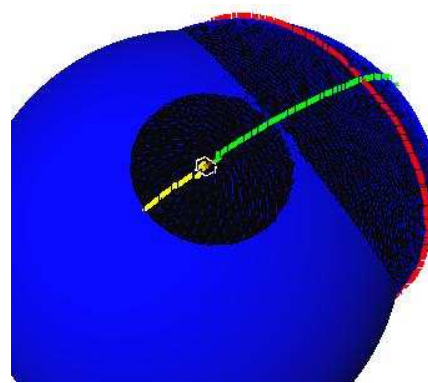
The variation of the  $b_0$  coefficient in the neighborhood of a blue ridge and a turning point of such a ridge are illustrated on Fig. 7. Summarizing the previous observations, we have:

**Definition. 6** *Let  $p \in M$  be a non-umbilical point, then  $p$  is a blue ridge point if one of the following equivalent conditions is satisfied:*

- (i) *the blue principal curvature has an extremum along the corresponding blue line of curvature,*
- (ii)  $b_0 = 0$ ,
- (iii) *the blue sphere of curvature has at least an  $A_3$  contact with  $M$  at  $p$ .*

Notice again that a contact involves a sphere and the surface. The contact therefore provides information on the surface but also on its focal surfaces—the blue/red one assuming the the sphere in contact is a principal blue/red sphere of curvature. The reader is referred to [BGG85] for local models of the focal at such singularities. We actually have the following:

**Observation. 3** *At a ridge point, the focal surface is not regular—the center of the osculating sphere is located on a cuspidal edge of the focal surface.*

Figure 8:  $A_2$  contact with the blue sphereFigure 9:  $A_2$  contact with the red sphereFigure 10:  $A_3^+$  contact of the blue sphere of curvature at a blue elliptic ridge point (on the blue curve)Figure 11:  $A_3^-$  contact of the blue sphere of curvature at a blue Hyperbolic ridge point (on the green curve)

#### 4.4 Contact points at umbilics

The Monge patch at an umbilic is of the following:

$$z = \frac{1}{2}k(x^2 + y^2) + \frac{1}{6}(b_0x^3 + 3b_1x^2y + 3b_2xy^2 + b_3y^3) + \frac{1}{24}(c_0x^4 + 4c_1x^3y + 6c_2x^2y^2 + 4c_3xy^3 + c_4y^4) + \dots$$

Note that away from umbilic, the  $x$  and  $y$  coordinates of the Monge coordinate system follow the principal directions; at the umbilic there is no such canonical choice of coordinates, hence the values of  $b_0 \neq 0$  and  $b_3 \neq 0$  are not relevant and other invariants must be considered.

To see which ones, consider the contact function given by Eq. (8). Since  $r = 1/k_1 = 1/k_2$ , it is dominated by the cubic terms. More precisely, the singularity is generically a  $D_4^\pm$ . The number of ridges passing through the umbilic is the number of curves in the zero level set of contact function. Hence this number reads on the normal form, and is equal to one or three as mentioned in observation 2. This fact is not intuitive and it is neither obvious that ridges pass through umbilics. A way to explain these facts is to study the gradient field  $\nabla k_1$  (the same holds for  $\nabla k_2$ ) well defined at non umbilical points. Indeed a non-umbilical blue ridge point can be seen as a point on a blue curvature line where  $\nabla k_1$  is orthogonal to the curve that is  $\nabla k_1 \cdot dmax = 0$ , or equivalently the iso-line of  $k_1$  is tangent to the curvature line. Hence one has to study orthogonality between the two fields  $\nabla k_1$  and  $dmax$ . In section 3.1, it has been shown that the index of the  $d_{max}$  fields distinguishes stars (index  $-1/2$ ) from lemons or monstars (index  $+1/2$ ). The study of  $k_1$  and  $\nabla k_1$  shows that generically, one has the following:

- $k_1$  has a minimum, then  $\nabla k_1$  has index 1; this also implies that the umbilic is a star and that there are 3 directions in which  $\nabla k_1 \perp dmax$  see Fig. 13;
- there is a curve along which  $k_1 = k$  is constant passing through the umbilic, then  $\nabla k_1$  has index 0 and there is 1 direction in which  $\nabla k_1 \perp dmax$  see Fig. 14.

The distinction between these two cases also reads on the Monge cubic  $C_M$ , its number of real factor lines is the number of ridges, hence it depends on the sign of its discriminant  $D = \delta(C_M)$ . One can summarize the previous discussion as follow:

**Theorem. 4** *Generic umbilics are of two types:*

- *Elliptic or 3-ridge umbilic. The Monge cubic has three different real factor lines, or equivalently the contact function has a  $D_4^-$  singularity, and three ridge lines cross at the umbilic. Moreover at the umbilic,  $k_1$  has a minimum and  $k_2$  a maximum. Such an umbilic is a star.*
- *Hyperbolic or 1-ridge umbilic. The Monge cubic has only one real factor line, or equivalently the contact function has a  $D_4^+$  singularity, and one ridge passes through the umbilic. Moreover passing through the umbilic, there are two curves along which  $k_1$  (resp.  $k_2$ ) is constant equal to  $k$ . Such an umbilic is either a lemon, a monstar or a star.*

The number of ridges is given by the number of real factors lines of the Monge cubic, but these lines are not the tangent directions to ridge lines going through the umbilic. However, these tangent directions can be computed from the Monge cubic cf. [HGY<sup>+</sup>99].

The intersection between the surface and its osculating sphere at an umbilic is not reduced to a point (cf. Observation 2). This fact remains true close to the umbilic and in particular on ridges, so we have:

**Observation. 4** *A ridge passing through an umbilic must be hyperbolic.*

It also turns out that ridges are smooth curves crossing transversally at the umbilic and changing color there —from a minimum of  $k_1$  to a maximum of  $k_2$ . Notice that a ridge may not pass through an umbilic, then it is of a single color and changes type at each turning point if any —there is an even number of such points.

**Rmk 2** A finer distinction of elliptic umbilics concerns the ordering of ridge colors around the umbilic: it is called *symmetrical* if ridges alternate colors  $RBRBRB$  (then  $T = b_0^2 + b_3^2 + 3(b_0b_2 + b_1b_3) < 0$ ) and *unsymmetrical* if the ordering is  $RRRBBB$  ( $T > 0$ ).

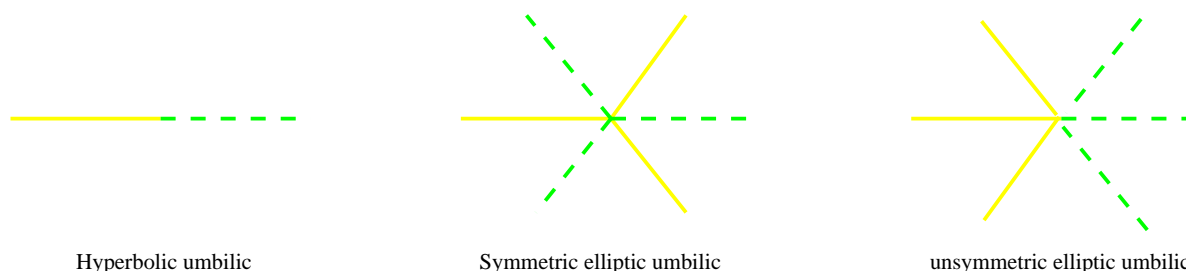


Figure 12: Ridges at umbilic

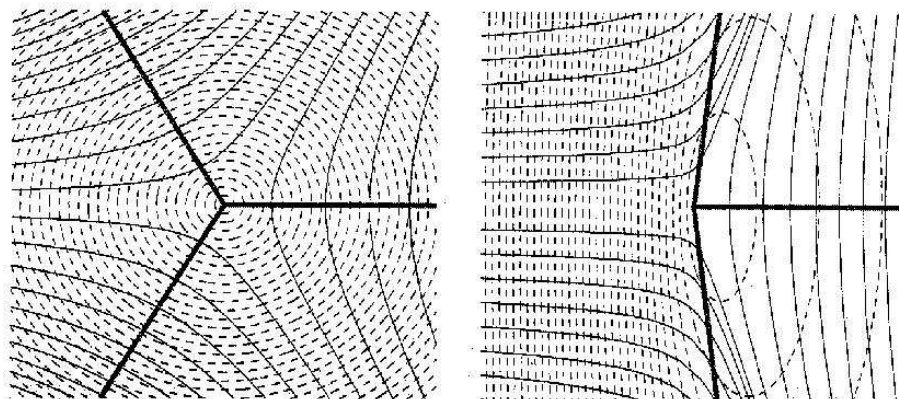


Figure 13: Elliptic umbilics are stars, either symmetric or unsymmetric. Dashed lines are level sets of the blue curvature, thin lines are blue curvature lines and thick lines are blue ridges. Note that a red ridge will continue each branch of the blue ridge, the color changes at the umbilic. The first picture features a symmetric umbilic and the second one an unsymmetric umbilic. Figure from [HGY<sup>+</sup>99].

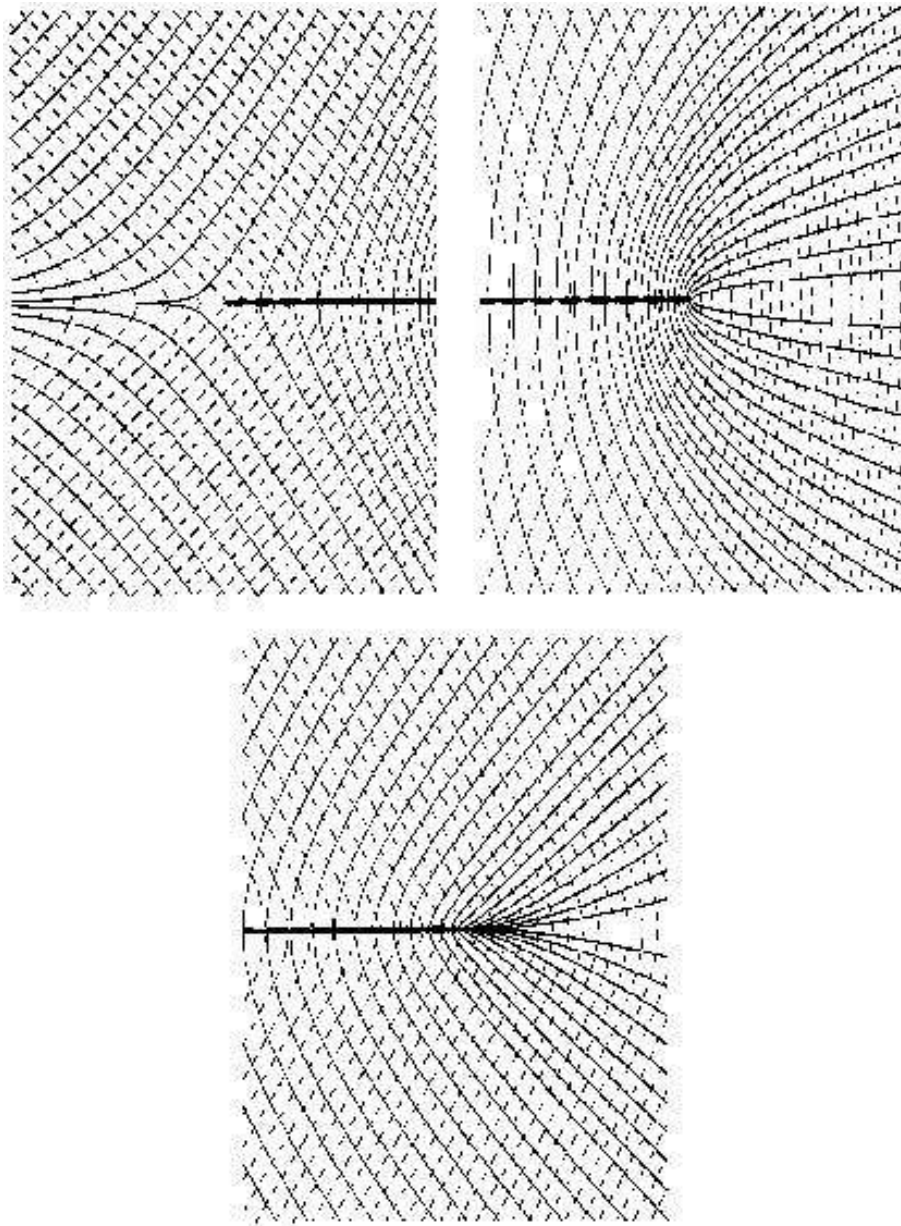


Figure 14: Hyperbolic umbilics: star, lemon and monstar. Dashed lines are level of the blue curvature, thin lines are blue curvature lines and thick lines are blue ridges. Figure from [HGY<sup>+</sup>99].

## 5 Medial axis, skeleton, ridges

### 5.1 Medial axis of a smooth surface

Given a closed manifold  $S$  embedded in  $\mathbb{R}^3$ , the medial axis  $MA(S)$  consists of the points of the open set  $\mathbb{R}^3 \setminus S$  having two or more nearest points on  $S$ . A related notion is the skeleton of  $\mathbb{R}^3 \setminus S$ , which consists of the centers of maximal spheres included in  $\mathbb{R}^3 \setminus S$ —maximal for the inclusion amongst such spheres. For smoothly embedded manifolds, the closure of the medial axis is actually equal to the skeleton, which is why we just refer to the medial axis in the sequel.

The medial axis has an outstanding position in many communities and has been rediscovered several times. Example relevant citation are [Erd46, Hor83] in analysis, [Tho72, Mil80] in differential geometry, [Ser82, Ser88, BA91, BA92] in mathematical morphology. Since we just aim at presenting the local and global structure of the medial axis, we shall follow [BGG85, GK00], but the interested reader should also consult [Yom81].

Having discussed the contact of a sphere with the surface, let us recall the classification of medial axis points and the corresponding *stratified* structure. While describing ridges, we actually cared more for the surface. For the medial axis, we change the perspective and care for the centers of the maximal spheres. When talking about a contact, one should therefore keep in mind that the corresponding sphere contributes its center to the medial axis.

Since we care for spheres intersecting the surface in an isolated point—otherwise the sphere is not contained in  $\mathbb{R}^3 \setminus S$ , the contact points must correspond to  $A_1^+$  and  $A_3^+$  singularities. Notice that an  $A_1^+$  singularity corresponds to a simple tangency. We shall drop the superscript and replace it by the *multiplicity* of the contact, that is  $A_1^k$  refers to a sphere having  $k$  separate  $A_1^+$  contacts. The medial axis points actually correspond to the following five cases:

- $A_1^4, A_1^3, A_1^2$  The sphere touches the surface at two, three or four points, and has a simple tangency at each contact point.  $A_1^4$  points are isolated points;  $A_1^3$  points lie on curves,  $A_1^2$  lie on sheets of the medial axis. Moreover, one has the following incidences. At an  $A_1^4$  point, six  $A_1^2$  sheets and four  $A_1^3$  curves meet. Along an  $A_1^3$  curve, three  $A_1^2$  sheets meet.
- $A_3^+$  The contact point is an elliptic ridge point. The corresponding medial axis points bound  $A_1^2$  sheets.
- $A_3^+ A_1$  The sphere has two contact points. The center of the sphere lies at the intersection between an  $A_1^3$  curve together with an  $A_3^+$  curve. This is where an  $A_1^2$  sheet vanishes.

An example is presented on Fig. 15. The top part looks like a chimney with triangular section and a void in the middle. Then the void vanishes and we are left with a cylinder of roughly triangular section. The section of the cylinder changes from triangular to roughly elliptic. Eventually, the cylinder splits into two legs of elliptic sections. Near the top, the structure of the medial axis is that of a tetrahedron, with six  $A_1^2$  sheets and four  $A_1^3$  curves meeting. The boundary of each sheet consists of an  $A_3$  curve. When the section gets rounder, one  $A_2$  sheet vanishes at an  $A_3 A_1$  point.

There is an intuitive way to understand the preceding results, by counting separately the numbers of degrees of freedom and the number of constraints attached to a particular medial axis point. To see how, recall that a contact involves one sphere and one or more points on the surface. In terms of degrees of freedom (dof), a sphere yields four degrees of freedom, choosing a point on a surface is another two dof, and choosing a point on a curve drawn on a surface is one dof. In terms of constraints at the contact points, constraining a sphere to have an  $A_1$  contact imposes three constraints. (Indeed the tangent plane being set to that of the surface at  $p$ , we are left with the choice of the radius —which defines the pencil of spheres through the contact point.) Similarly, having an  $A_3$  contact imposes four degrees of freedom since the radius of the sphere has to be one of the principal curvatures. Let us now discuss the different cases:

- $A_1^2$  Having two contacts of order one imposes  $2 \cdot 3 = 6$  constraints. But choosing two points on  $S$  together with the contact spheres yields  $2 \cdot 2 + 4 = 8$  dof. One can expect  $A_1^2$  points to lie on sheets.
- $A_1^3$  Three  $A_1$  contacts define  $3 \cdot 3 = 9$  constraints, and  $3 \cdot 2 + 4 = 10$  dof.  $A_1^3$  points are expected to lie on curves.
- $A_1^4$  Four  $A_1$  yield  $4 \cdot 3 = 12$  constraints and  $4 \cdot 2 + 4 = 12$  dof. These medial axis points are expected to be isolated.
- $A_3$  Such a point yields 4 constraints. In terms of dof, and since  $A_3$  points lie on curves on the surface, we have one dof for the choice of the contact point, and four for the sphere.  $A_3$  contacts are therefore expected along curves.
- $A_3A_1$  The contact points respectively yield  $4 + 3$  constraints. On the other hand, choosing one point along a curve, another on the surface, together with the dof of the sphere yield  $2 + 1 + 4$  dof. Such contacts are expected to be isolated.

## 5.2 Medial axis and ridges

Spheres centered on the boundary of the medial axis project onto elliptic ridge points of type  $A_3^+$  on the surface. But an elliptic ridge point can fail to be the contact of a point of the boundary of the MA in two cases: (i) if the limiting bitangent sphere crosses the surface away from the ridge point or (ii) if the surface is locally inside this sphere. (This latter case happens in elliptic regions for a positive minimum of  $k_2$  or a negative maximum of  $k_1$ ). In the first case, the sphere is not contained in  $\mathbb{R}^3 \setminus S$ , and in the second it is not maximal for inclusion.

Fig. 16 illustrates case (i), the lowest point is an elliptic ridge point but its bitangent sphere has a non local intersection with the curve. Fig. 1 illustrates case (ii), the blue elliptic ridge is the loci of negative maximum of  $k_1$ . The MA, which is an ellipsoid in the equatorial plane (spanned by the two longest principal axis of the ellipsoid), only gives birth to the red ridge (negative minimum of  $k_2$ ).

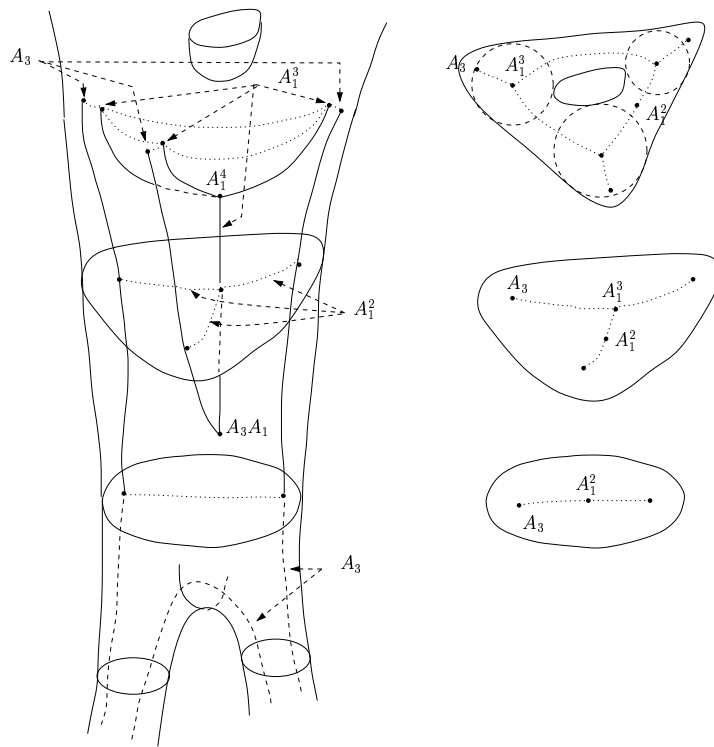


Figure 15: The stratified structure of the medial axis of a smooth surface



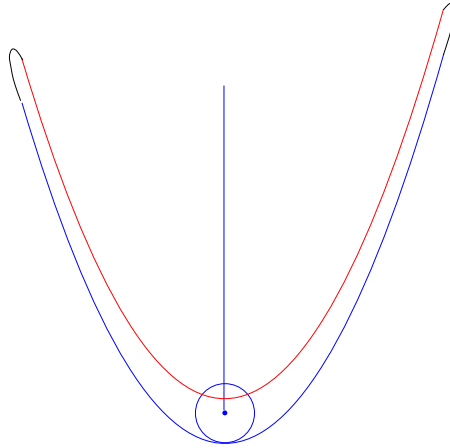


Figure 16: An extrema of curvature not image of the medial axis boundary

## 6 Conclusion

We surveyed the notions of umbilics, lines of curvatures, foliations, ridges and medial axis for smooth surfaces, with an emphasis on global structure theorems.

An important aspect which has been eluded is the dynamic case, that is the structure theorems valid if one replace a surface by say a one-parameter family of surfaces. Of particular interest in that case are the birth and death phenomena. These indeed feature transitions between patterns observed in the static case, and the time events between them are a measure of persistence of the objects involved. The reader is referred to [BG86, GK02, BGT96] [HGY<sup>+</sup>99, chap.7] for pointers in that direction concerning ridges and MA. Note that it does not make sense to study a single line of curvature dynamically. One has to consider the topology of the principal foliation instead, this is usually referred as bifurcation theory, see [Tri02].

## 7 Appendix: Umbilic classification in the complex plane

The classification of umbilics with respect to the cubic part of the Monge form of the surface can be illustrated by a diagram in the plane (Fig. 17). With a change of variables which corresponds to a rotation in the tangent plane and noting  $\zeta = x + iy$  the cubic form  $b_0x^3 + 3b_1x^2y + 3b_2xy^2 + b_3y^3$  becomes  $Re(\zeta^3 + \omega\zeta^2\bar{\zeta})$  for some complex number  $\omega$ . Then umbilics are parameterized by  $\omega$  in the complex plane. The zero sets of the four invariants  $S, U, D$  and  $T$  give four curves partitioning the plane in sectors. Umbilics on the complement of these curves are generic.

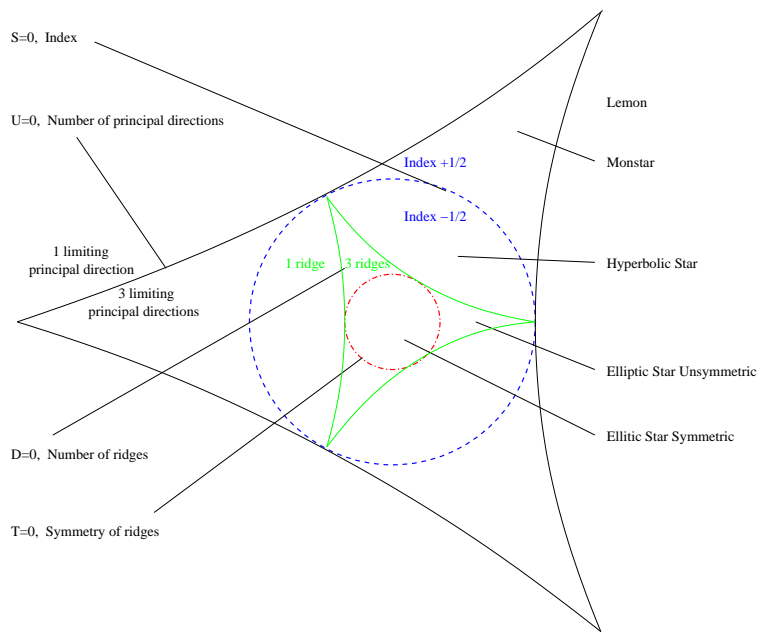


Figure 17: Umbilic classification in the complex plan

## References

- [AB99] Nina Amenta and Marshall Bern. Surface reconstruction by Voronoi filtering. *Discrete Comput. Geom.*, 22(4):481–504, 1999.
- [ACDL00] N. Amenta, S. Choi, T. K. Dey, and N. Leekha. A simple algorithm for homeomorphic surface reconstruction. In *Proc. 16th Annu. ACM Sympos. Comput. Geom.*, pages 213–222, 2000.
- [ACSD<sup>+</sup>03] Pierre Alliez, David Cohen-Steiner, Olivier Devillers, Bruno Levy, and Mathieu Desbrun. Anisotropic polygonal remeshing. *ACM Transactions on Graphics*, 2003. SIGGRAPH '2003 Conference Proceedings.
- [Arn92] V.I. Arnold. *Catastrophe theory (3rd Ed.)*. Springer, 1992.
- [BA91] Jonathan W. Brandt and V. Ralph Algazi. Computing a stable, connected skeleton from discrete data. In *Proceedings of the 1991 IEEE Computer Society Conference on Computer Vision and Pattern Recognition*, pages 666–667, IEEE Service Center, Piscataway, NJ, USA (IEEE cat n 91CH2983-5), 1991. IEEE.
- [BA92] J. W. Brandt and V. R. Algazi. Continuous skeleton computation by Voronoi diagram. *CVGIP: Image Understanding*, 55(3):329–338, 1992.
- [BC01] J.-D. Boissonnat and F. Cazals. Natural neighbor coordinates of points on a surface. *Comput. Geom. Theory Appl.*, 19:155–173, 2001.
- [BCM03] V. Borrelli, F. Cazals, and J-M. Morvan. On the angular defect of triangulations and the pointwise approximation of curvatures. *Comput. Aided Geom. Design*, 20, 2003.
- [BCSV04] J.-D. Boissonnat, D. Cohen-Steiner, and G. Vegter. Meshing an implicit surface with certified topology. In *ACM STOC*, 2004.
- [BG86] J. Bruce and P. Giblin. Growth, motion and 1-parameter families of symmetry sets. *Proc. R. Soc. Edinb., Sect. A*, 104, 1986.
- [BG92] J.W. Bruce and P.J. Giblin. *Curves and singularities (2nd Ed.)*. Cambridge, 1992.
- [BGG85] J. Bruce, P. Giblin, and C. Gibson. Symmetry sets. *Proc. Roy Soc Edinburgh Sect. A*, 101, 1985.
- [BGT96] J. Bruce, P. Giblin, and F. Tari. Ridges, crests and sub-parabolic lines of evolving surfaces. *Int. J. Computer Vision*, 18(3):195–210, 1996.
- [BO03] J.-D. Boissonnat and S. Oudot. Provably good surface sampling and approximation. In *Symp. on Geometry Processing*, 2003.
- [CCs04] F. Chazal and D. Cohen-steiner. A condition for isotopic approximation. In *ACM Symposium on Solid Modeling*, 2004.

- [CP03] F. Cazals and M. Pouget. Estimating differential quantities using polynomial fitting of osculating jets. In *Symp. on Geometry Processing*, 2003.
- [CP04] F. Cazals and M. Pouget. Differential loci on sampled smooth surfaces: an algorithmic roadmap. *Work in process*, 2004.
- [CSM03] D. Cohen-Steiner and J.-M. Morvan. Restricted delaunay triangulations and normal cycle. In *ACM Symposium on Computational Geometry*, 2003.
- [Deg97] W. L. F. Degen. The cut locus of an ellipsoid. *Geometriae Dedicata*, 67(2), 1997.
- [DH94] T. Delmarcelle and L. Hesselink. The topology of symmetric, second-order tensor fields. In *IEEE Visualization Proceedings*, pages 104–145, 1994.
- [DZ02] T. K. Dey and W. Zhao. Approximate medial axis as a voronoi subcomplex. In *ACM Sympos. Solid Modeling and Applications*, 2002.
- [Erd46] P. Erdős. On the hausdorff dimension of some sets in euclidean space. *Bull. Am. Math. Soc.*, 52, 1946.
- [GK00] P. Giblin and B. Kimia. A formal classification of 3d medial axis points and their local geometry. In *Computer Vision and Pattern Recognition*, Hilton Head, South Carolina, USA, 2000.
- [GK02] P. Giblin and B. Kimia. Transitions of the 3d medial axis under a one-parameter family of deformations. *ECCV*, 1, 2002.
- [GS91] C. Gutierrez and J. Sotomayor. *Lines of Curvature and Umbilical Points on Surfaces*. IMPA, 1991.
- [HGY+99] P. W. Hallinan, G. Gordon, A.L. Yuille, P. Giblin, and D. Mumford. *Two-and Three-Dimensional Patterns of the Face*. A.K.Peters, 1999.
- [Hor83] L. Hormander. *The analysis of linear partial differential operators - I*. Springer, 1983.
- [Lie03] A. Lieutier. Any open bounded subset of  $\mathbb{R}^n$  has the same homotopy type than its medial axis. In *ACM Solid Modeling*, 2003.
- [Mil80] D. Milman. The central function of the boundary of a domain and its differentiable properties. *J. Geom.*, 14, 1980.
- [Mor90] R. Morris. *Symmetry of curves and the geometry of surfaces: two explorations with the aid of computer graphics*. PhD thesis, Univ. of Liverpool, 1990.
- [MT01] J-M. Morvan and B. Thibert. Smooth surface and triangular mesh : Comparison of the area, the normals and the unfolding. In *ACM Symposium on Solid Modeling and Applications*, 2001.

- [Nik01] I. Nikolaev. *Foliations on Surfaces*. Springer, 2001.
- [PAT00] X. Pennec, N. Ayache, and J.-P. Thirion. Landmark-based registration using features identified through differential geometry. In I. Bankman, editor, *Handbook of Medical Imaging*. Academic Press, 2000.
- [Pet01] S. Petitjean. A survey of methods for recovering quadrics in triangle meshes. *ACM Computing Surveys*, 34(2), 2001.
- [Por71] I. Porteous. The normal singularities of a submanifold. *J. Diff. Geom.*, 5, 1971.
- [Por83] I. Porteous. Normal singularities of surfaces in  $\mathbb{R}^3$ . In *Proc. Symp. Pure Math. (40, Part II)*, 1983.
- [Por01] I. Porteous. *Geometric Differentiation (2nd Edition)*. Cambridge University Press, 2001.
- [PS03] T. Peters and T. Sakkalis. Ambient isotopic approximations for surface reconstruction and interval solids. In *ACM Symposium on Solid Modeling*, 2003.
- [Ser82] J. Serra. *Image Analysis and Mathematical Morphology*. Academic Press, London, UK, 1982.
- [Ser88] J. Serra, editor. *Image Analysis and Mathematical Morphology, volume 2: Theoretical Advances*. Academic Press, New York, 1988.
- [Spi99] M. Spivak. *A Comprehensive Introduction to Differential Geometry*, volume 3. Publish or perish, 1999.
- [Tho72] R. Thom. Sur le cut-locus d'une variété plongeée. *J. Differ. Geom.*, 6, 1972.
- [Tri02] X. Tricoche. *Vector and Tensor Field Topology Simplification, Tracking, and Visualization*. Universitat Kaiserslautern, 2002.
- [WB01] K. Watanabe and A.G. Belyaev. Detection of salient curvature features on polygonal surfaces. In *Eurographics*, 2001.
- [Yom81] Y. Yomdin. On the general structure of a generic central set. *Compositio Math*, 43, 1981.

## Contents

<b>1</b>	<b>Introduction</b>	<b>3</b>
1.1	Global differential patterns . . . . .	3
1.2	An example: the ellipsoid . . . . .	4
1.3	Paper overview . . . . .	5
<b>2</b>	<b>The Monge form of a surface</b>	<b>5</b>
2.1	Generic surfaces . . . . .	5
2.2	The Monge form of a surface . . . . .	5
<b>3</b>	<b>Umbilics and lines of curvature, principal foliations</b>	<b>6</b>
3.1	Classification of umbilics . . . . .	7
3.2	Principal foliations . . . . .	9
<b>4</b>	<b>Contacts of the surface with spheres, Ridges</b>	<b>11</b>
4.1	Distance function and contact function . . . . .	11
4.2	Generic contacts between a sphere and a surface . . . . .	11
4.3	Contact points away from umbilics . . . . .	13
4.4	Contact points at umbilics . . . . .	15
<b>5</b>	<b>Medial axis, skeleton, ridges</b>	<b>19</b>
5.1	Medial axis of a smooth surface . . . . .	19
5.2	Medial axis and ridges . . . . .	20
<b>6</b>	<b>Conclusion</b>	<b>22</b>
<b>7</b>	<b>Appendix: Umbilic classification in the complex plane</b>	<b>22</b>



---

Unité de recherche INRIA Sophia Antipolis  
2004, route des Lucioles - BP 93 - 06902 Sophia Antipolis Cedex (France)

Unité de recherche INRIA Futurs : Parc Club Orsay Université - ZAC des Vignes  
4, rue Jacques Monod - 91893 ORSAY Cedex (France)

Unité de recherche INRIA Lorraine : LORIA, Technopôle de Nancy-Brabois - Campus scientifique que  
615, rue du Jardin Botanique - BP 101 - 54602 Villers-lès-Nancy Cedex (France)

Unité de recherche INRIA Rennes : IRISA, Campus universitaire de Beaulieu - 35042 Rennes Cedex (France)

Unité de recherche INRIA Rhône-Alpes : 655, avenue de l'Europe - 38334 Montbonnot Saint-Ismier (France)

Unité de recherche INRIA Rocquencourt : Domaine de Voluceau - Rocquencourt - BP 105 - 78153 Le Chesnay Cedex (France)

---

Éditeur  
INRIA - Domaine de Voluceau - Rocquencourt, BP 105 - 78153 Le Chesnay Cedex (France)

<http://www.inria.fr>

ISSN 0249-6399